Measurement of the ^{230}Th$(p, 2n)$ ^{229}Pa and ^{230}Th$(p, 3n)$ ^{228}Pa reaction cross sections from 14.1 to 16.9 MeV

Kelly N. Kmak [1,2,*] Dawn A. Shaughnessy,[2] and Jasmina Vujic [1]

[1]*Nuclear Engineering Department, University of California Berkeley, Berkeley, California 94720, USA*

[2]*Lawrence Livermore National Laboratory, Nuclear and Chemical Sciences Division, Livermore, California 94550, USA*

(Received 26 January 2021; accepted 3 March 2021; published 15 March 2021)

Background: Actinium-225 is of interest for medical isotope production and there is on-going research into methods of producing ^{225}Ac, either directly or via the decay of its parent isotopes (^{229}Th, ^{229}Pa, and ^{225}Ra). One method that has been suggested is the ^{230}Th$(p, 2n)$ ^{229}Pa reaction. However, there is no available cross-section data for this reaction in the literature.

Purpose: Measure the ^{230}Th$(p, 2n)$ and ^{230}Th$(p, 3n)$ reaction cross sections in the energy range where the $(p, 2n)$ reaction is predicted to peak to determine the feasibility of ^{225}Ac production via the ^{230}Th$(p, 2n)$ reaction.

Methods: Targets naturally enriched in ^{230}Th were irradiated at the Center for Accelerator Mass Spectrometry at Lawrence Livermore National Laboratory with energies ranging from 14.1 to 16.9 MeV. Chemical processing was used to separate the protactinium activation products, followed by γ-ray spectroscopy to measure the activities of ^{228,229,230,232}Pa produced in the irradiation.

Results: Excitation functions are reported for the first time in the literature for the ^{230}Th$(p, 2n)$ and ^{230}Th$(p, 3n)$ reactions in this energy range. The peak measured value of the ^{230}Th$(p, 2n)$ reaction was found to be 182 ± 12 mb at 14.4 ± 0.1 MeV. The ^{232}Th(p, n) ^{232}Pa reaction was used to verify the experimental conditions, the measured values are reported and are comparable to the existing literature values. From the γ-ray spectrometry data, the half-life of ^{229}Pa was measured as 1.5 ± 0.1 days, which is within the error of the half-life reported in the evaluated nuclear data as well as in the recent measurements, and the half-life of ^{228}Pa was measured as 19.5 ± 0.4 hours.

Conclusions: The ^{230}Th$(p, 2n)$ ^{229}Pa reaction could reasonably be used for ^{225}Ac isotope production, although significant amounts of relatively isotopically pure ^{230}Th would be needed for significant production because the low alpha-decay branching ratio of ^{229}Pa and long half-life of ^{229}Th inhibit the in-growth of significant amounts of ^{225}Ac.

DOI: 10.1103/PhysRevC.103.034610

I. INTRODUCTION

Actinium-225 shows enormous potential for use in targeted alpha therapy (TAT) for cancer treatment [1]. Clinical trials have been done on the use of ^{225}Ac to treat leukemia [2]; it has shown efficacy in the treatment of prostate cancer [3], and ovarian cancer treatment has been investigated with animal studies [4]. The ^{213}Bi daughter of ^{225}Ac has also been studied for use as a TAT agent [5–7] and used successfully in the treatment of patients with neuroendocrine tumors [8].

Currently, ^{225}Ac for clinical trials is obtained from the decay of ^{229}Th (Fig. 1), a long-lived daughter of ^{233}U, a fissile isotope produced in nuclear programs for weapons and reactors [9–11]. However, the current supply is not sufficient to allow for extensive use, or even trials, of ^{225}Ac [9,10]. Due to a combination of scientific and regulatory constraints, it is impractical to produce ^{233}U in sufficient quantities to meet the current demands for ^{225}Ac [9]. Therefore, research is being done on alternative methods of ^{225}Ac production to meet current and future demands.

Production of ^{225}Ac and its parent ^{229}Th via reactions on ^{230}Th, particularly the $(n, 2n)$, (γ, n), $(p, 2n)$, and $(p, 2p)$ reactions, has been considered [11,12]. However, there is limited nuclear data available on ^{230}Th reaction cross sections. While the neutron-induced fission of ^{230}Th has been well studied [13–15] and studies have used proton bombardment on ^{230}Th to probe the nuclear structure of ^{229}Pa [16,17] and ^{227}Ac [18], there is no ^{230}Th(p, xn) reaction cross-section data available in the literature. The goal of this work is to present data on measurements of the ^{230}Th$(p, 2n)$ ^{229}Pa reaction cross section to gauge the feasibility of using this reaction for ^{225}Ac production via the decay of ^{229}Pa (Fig. 1). Because the ^{230}Th$(p, 2n)$ reaction has been predicted to peak around 14 to 15 MeV [17,19], this study will focus on measuring the cross section between 14 and 17 MeV. A limited portion of the excitation function of the ^{230}Th$(p, 3n)$ reaction, which has a threshold at 15 MeV [20,21], was also measured in this energy region.

While the availability of ^{230}Th is limited [12], it can be obtained from uranium or uranium ore-byproducts [12,23,24] because it is naturally occurring in the ^{238}U decay chain. The ^{230}Th used in this work was separated from a high-grade uranium ore (39.1 ± 1.8 wt.% uranium) [24]. Because it is

*kmak1@llnl.gov

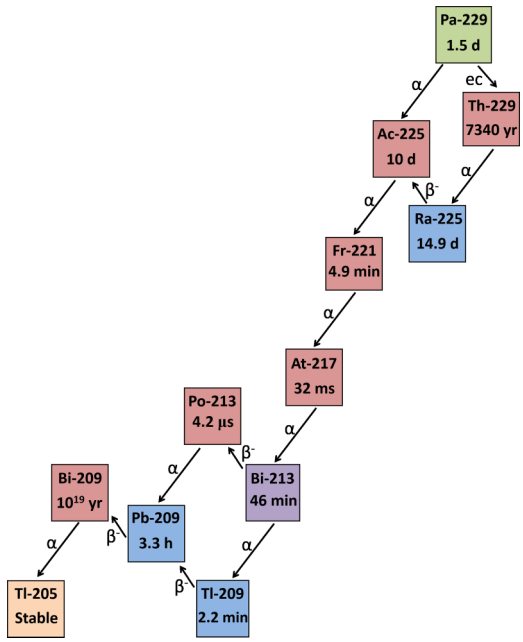

FIG. 1. Decay chain of ^{229}Pa, data from Ref. [22].

naturally occurring, the target material contains both ^{232}Th and ^{230}Th. However, due to the high uranium and low "natural thorium" (^{232}Th) content of the ore, the thorium material is naturally enriched in ^{230}Th with a ^{230}Th / ^{232}Th isotope ratio of 0.0922 ± 0.00150, several orders of magnitude larger than the ^{230}Th / ^{232}Th isotope ratios in typical minerals, which are on the order of 10^{-6} to 10^{-5} [25,26]. To ensure there was no interference from the ^{232}Th$(p, 4n)^{229}$Pa reaction, all irradiations were conducted well below the threshold for that reaction (19.5 MeV) [11,20,21]. The ^{232}Th$(p, n)^{232}$Pa reaction cross section, which is fairly well known and has no interfering reaction from ^{230}Th, was measured simultaneously with the ^{230}Th$(p, 2n)$ and ^{230}Th$(p, 3n)$ reactions for all measurements to validate the experimental conditions.

Cross-section measurements were made with three proton irradiations at varying energies and the excitation functions for the ^{230}Th$(p, 2n)^{229}$Pa, ^{230}Th$(p, 3n)^{228}$Pa, and ^{232}Th$(p, n)^{232}$Pa reactions are reported from 14.1 to 16.9 MeV. The excitation functions for the ^{230}Th$(p, 2n)^{229}$Pa and ^{230}Th$(p, 3n)^{228}$Pa reactions reported here have not been previously presented in the literature. The cross-section results are compared with the theoretical calculations from TENDL 2019 [19], the output library of the nuclear code TALYS, as well as existing nuclear data for the ^{232}Th(p, n) reaction. The half-lives of ^{229}Pa and ^{228}Pa were also measured and the data are presented.

II. EXPERIMENTAL WORK

A. Irradiation facility

The irradiations were performed at the Center for Accelerator Mass Spectrometry (CAMS) at Lawrence Livermore National Laboratory (LLNL) with a 10 MV tandem accelerator. Three irradiations were performed over several months

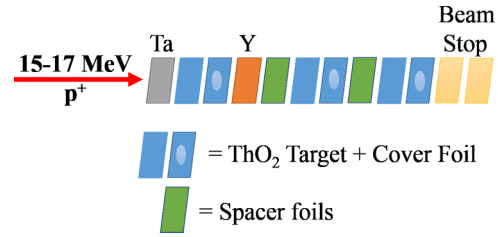

FIG. 2. Schematic of the target stack for each of the irradiations. Targets, cover foils, and spacer foils are described in Sec. II B. The first irradiation had no spacer foils and only two target foils.

with proton energies of 15, 16, and 17 MeV. Beam currents ranged from 185 ± 7 to 277 ± 13 nA. The irradiations ranged from 8 to 12 hours in length. The thorium targets, cover foils, and spacer foils were stacked into an aluminum holder that was mounted in the CAMS irradiation chamber; the targets and foils were trimmed to 8 mm squares to fit in the holder. During the irradiations, the chamber was under vacuum and the beam stop was water cooled.

B. Targets

Thorium oxide targets were fabricated with thorium obtained from natural uranium ore (details of the ore and the separation procedure are given in Ref. [24]). The ^{230}Th / ^{232}Th isotope ratio, as mentioned previously, was 0.0922 ± 0.00150, as determined by mass spectrometry [24]. The target-backing material was 10 μm light-tested (LT) titanium (99.9%, Goodfellow). Target thicknesses ranged from 921.710 ± 0.005 to 1913.309 ± 0.005 μg Th/cm^2. Total target mass was determined with γ-ray spectrometry using the 67 keV γ-ray line of ^{230}Th, and target uniformity was determined with a position-sensitive alpha detector.

A total of eight thorium targets were irradiated and processed over three irradiations. The proton energy through the target stack was modeled using the program SRIM 2013 [27]. Spacer foils of tantalum (10 μm, 99.9%, LT, Goodfellow) and platinum (25 μm, 99.99+%, LT, Goodfellow) were used to degrade the energy and allow the cross sections to be determined over a range of energies ($\approx$1 MeV) per irradiation. Thin titanium (2 μm, 99.99%, Lebow Company) cover foils were positioned in front of each target during the irradiations and then chemically processed with their respective target. A yttrium foil (5 μm, 99%, Goodfellow, not light tested) was used as a flux monitor for all irradiations and a thin tantalum foil (5 μm, 99.9%, Goodfellow, not light tested) was the first foil in each stack as per the irradiation facility guidelines. The target stack is shown in Fig. 2.

C. Target processing

Target processing was necessary to detect the protactinium activation products over the high background from fission products and titanium activation products. After each irradiation, the targets were removed from the CAMS beamline within an hour and brought to a laboratory for chemical processing. Each target foil and its cover foil were removed from the target stack and placed in separate 5 mL plastic tubes. To

each target, 1000 μL conc. HCl and 10 μL of a ^{233}Pa tracer ($\approx$1000 dps) in conc. HF were added to dissolve the target and backing material. A standard solution containing only the ^{233}Pa tracer was made in the same manner.

After the dissolution was complete (1.5 hours), column chromatography was used to separate protactinium. The target solutions and standard were diluted with 148 μL $AlCl_3$ (2.741 M), 666 μL conc. HCl, and 176 μL water, giving a final concentration of 10 M HCl : 0.14 M HF : 0.2 M $AlCl_3$. For each target solution, a 2 mL Dowex 1 × 8 (100–200 mesh) column was prepared and washed with 8 mL 10 M HCl. After the wash, the target solutions were loaded into the columns with two 500 μL rinses of the empty tube. All fractions were collected in 2 mL increments: six fractions of 10 M HCl, followed by seven fractions of 6 M HCl, and finally four fractions of 9 M HCl : 0.1 M HF. Protactinium eluted mainly in fraction 15, which had a radiopurity of >99% and a protactinium yield of 63 ± 1% to 85 ± 6%, as determined from the ^{233}Pa tracer, with the higher mass targets having lower chemical yields. The remainder of the protactinium was in fractions 14 and 16 as well as the empty tube ($\approx$5%–10%). After the separation, the protactinium samples were counted with γ-ray spectrometry. The total time from the end of the irradiation to the start of the γ-ray spectroscopy of the separated protactinium samples was about 8 hours. For each target, fraction 15 was used for all protactinium activity measurements.

Protactinium-233 was chosen as the yield tracer because it has several strong γ-ray lines [22] and its production from nuclear reactions in the target is negligible because the ^{232}Th(p, γ) reaction cross section is small (<400 μb) in this energy range [28,29] and there is no route to ^{233}Pa from ^{230}Th.

For the targets irradiated at higher energies (>16 MeV), the significant ^{230}Pa production necessitated further chemical processing to measure the ^{213}Bi daughter of ^{229}Pa (Fig. 1) with reasonable counting statistics because ^{230}Pa (440.78 keV) and ^{213}Bi (440.45 keV) have γ-ray emissions with similar energies (see Table S1 in the Supplemental Material [30] for a complete table of half-lives and relevant γ-ray energies and intensities) [22]. For these samples, protactinium and actinium were separated with column chromatography 35 days post-irradiation. The samples were evaporated to dryness and reconstituted in 2 mL of 10 M HCl : 0.14 M HF : 0.2 M $AlCl_3$, the same load solution as used for the initial separation. As before, the separations were performed with 2 mL Dowex 1 × 8 (100–200 mesh) columns, which had been prepared and washed with 8 mL 10 M HCl. Samples were loaded onto the columns with two 500 μL rinses of the empty tube.

All fractions were collected in 2 mL increments: four fractions of 10 M HCl, followed by four fractions of 9 M HCl : 0.1 M HF. The average total yield of actinium on this column was 99 ± 2%, as determined from three studies with tracer isotopes (^{233}Pa, ^{228}Ac) under identical chemical conditions. While the yield was high, actinium eluted in a broad band over most fractions. As before, the cleanest fraction was selected for γ-ray spectrometry, which was fraction 1 with an average actinium yield of 45.6 ± 0.2%.

The actinium samples were counted with γ-ray spectrometry after a decay period of 12 hours, which ensured that ^{213}Bi and ^{221}Fr were in equilibrium with ^{225}Ac. For the targets irradiated at lower energies, there was far less ^{230}Pa produced and, therefore, the in-growth of ^{213}Bi could be measured without further chemical processing. The 218.0 keV line from ^{221}Fr was also visible in some of the samples but it was not present with reasonable counting statistics and not used quantitatively.

D. Gamma-ray spectrometry

The chemical yield was determined with relative γ-ray spectroscopy. Each separated protactinium sample was counted relative to the ^{233}Pa standard immediately after chemical processing with a HPGe detector with Ortec NIM electronics and an ASPEC multichannel analyzer. Maestro software (Ortec) was used to analyze the resultant spectra. All samples and the standard were counted in the same geometry.

To make the cross-section measurement, the protactinium samples were counted with γ-ray spectrometry at the Nuclear Counting Facility (NCF) at LLNL. All samples were counted with a HPGe detector as well as a low-energy photon spectrometer (LEPS) detector. The detectors were calibrated with a ^{152}Eu source and the code GAMANAL [31] was used to analyze the resultant spectra. Each sample was counted at approximately 10 hours post-irradiation with the LEPS detector. Gamma-ray spectra were taken with the HPGe detector at approximately 12, 18, 24, 36, and 48 hours post-irradiation followed by additional counts every 24 hours for the next 6 days. The yttrium flux monitor foil was counted with the HPGe detector immediately with two spectra measured within four hours post-irradiation. Samples were recounted with the HPGe detector, either with or without prior chemical processing, about 35 to 40 days post-irradiation.

For all protactinium samples, the activities of ^{233}Pa, ^{232}Pa, ^{230}Pa, and ^{229}Pa were determined as well as ^{228}Pa, if present. The activities of ^{233,232,230,228}Pa can be readily determined with γ-ray spectrometry because these isotopes have several high-intensity lines (see Table S1 in the Supplemental Material [30]). As ^{229}Pa has only weak, low energy γ-ray lines, the LEPS detector was used in conjunction with repeated counts on the HPGe detector over several ^{229}Pa half-lives to make a direct activity measurement. X-ray analysis of each spectrum as well as measurements of the in-growth of its daughter, ^{213}Bi, were used to confirm the activity.

From the γ-ray spectrometry data, the activity of each isotope at the end of the irradiation (A_0) can be determined with the known, absolute intensities of its γ-ray lines and a decay correction based on the half-life and the time since the irradiation ended. From A_0, the cross section can be calculated with Eq. (1), where σ is the microscopic cross section (cm^2), nx is the areal density of the target material (atoms/cm^2), I is the current (protons/s), t is the irradiation time (s), and λ is the decay constant (s^{-1}) of the isotope of interest:

$$A_0 = \sigma n x I (1 - e^{-\lambda t}). \quad (1)$$

The activity of ^{89}Zr in the yttrium flux monitor foil was used to determine the current using Eq. (1) with the known cross section of the ^{89}Y(p, n) ^{89}Zr reaction [32]. Isotope decay during counting was not relevant for any of the γ-ray spectrometry measurements.

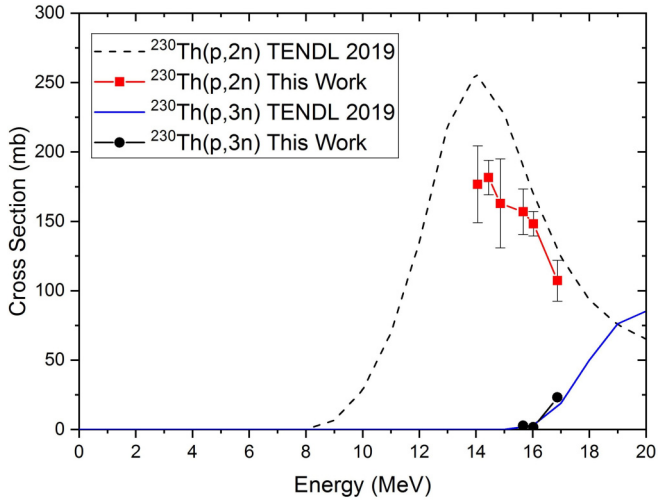

FIG. 3. Measured excitation functions of the ^{230}Th$(p, 2n)$ ^{229}Pa and ^{230}Th$(p, 3n)$ ^{228}Pa reactions from 14.1 to 16.9 MeV compared with the TENDL 2019 calculations. Cross-section error propagated from the standard deviation of several activity measurements. The point at 15.66 ± 0.15 MeV is an average over three measurements; the error on the cross section and the energy is given by the standard deviation.

III. RESULTS AND DISCUSSION

A. Cross-section measurements

The cross-section data were gathered over three separate irradiations with a total of eight thorium targets. For each target, the ^{232}Th(p, n), ^{230}Th$(p, 2n)$, and ^{230}Th$(p, 3n)$ cross sections were measured simultaneously. For all cross-section measurements, the error was propagated from the standard deviation of several activity measurements (3%–19%) as well as error from the calibration of the detectors (≈1%–5%), beam current (≈4%), target thickness (≈2%), and chemical yield (≈4%). There is a standard error of 0.1 MeV on the projectile energy based on the irradiation facility conditions and SRIM modeling of the energy through the target stack. Six separate cross-section measurements are shown for each reaction as three of the eight targets were irradiated at an energy of 15.66 ± 0.15 MeV (error from the standard deviation). For this energy, the cross section was calculated from the average of the three measurements with the error given by the standard deviation.

The excitation functions for the ^{230}Th$(p, 2n)$ ^{229}Pa and ^{230}Th$(p, 3n)$ ^{228}Pa reactions are shown in Fig. 3 and all cross-section data are given in Table I. The average ^{228}Pa activity was determined based on its 338, 409, and 911 keV lines in three spectra taken within the first 24 hours post-irradiation; the error is from the standard deviation. The ^{229}Pa activity was determined from its 119 keV γ-ray line [22,33]. As this is a weak emission (see Table S1 and Fig. S1 in the Supplemental Material [30]), γ-ray spectra were taken with the HPGe and LEPS detectors five times over the 36 hours post-irradiation and the activity determined from the average and standard deviation of these measurements. Because the activity measurement was based on one line, x-ray analysis and measurements of the in-growth of ^{213}Bi were also done to confirm the activity measurement. For each protactinium sample, the x rays in the five γ-ray spectra, mentioned previously, were also analyzed for their activity, interferences, and decay rate of the five protactinium isotopes present (^{228,229,230,232,233}Pa), taking into account five to six major x-ray energies for each isotope as well as low energy (<150 keV) γ-ray lines. The energy range was chosen to ensure the activities of ^{228,230,232,233}Pa could be determined separately with data from their higher-energy γ-ray lines, particularly ^{232}Pa which has a 150 keV line with a significant intensity [22]. The ^{229}Pa activity calculated from the x-ray analysis was within the error of the direct activity measurement (Fig. 4) except for the measurement at 16.9 MeV, where the x-ray result was higher. This is likely due to increased interferences at higher energies as the ^{232}Th(p, f) and ^{232}Th$(p, 3n)$ cross sections increase considerably as the energy increases. The in-growth of ^{213}Bi into the protactinium samples, as determined by γ-ray spectrometry 35 to 40 days post-irradiation, confirmed the direct activity measurement as well.

The peak of the ^{230}Th$(p, 2n)$ excitation function is between 14 and 15 MeV but cannot be determined more precisely from this data because the cross-section measurements at 14.1, 14.4, and 14.9 MeV are all within error. However, the general shape of the excitation function can be seen because there is a clear decrease in the cross section from 14.1 to 16.9 MeV. The maximum measured cross section was 182 ± 12 mb at 14.4 ± 0.1 MeV. The ^{230}Th$(p, 3n)$ cross section is low in this region, which is expected because the threshold is at 15.0 MeV [20,21], but it is clearly increasing as the energy increases. Due to the high threshold relative to the energy region studied, only three cross sections were measured for this reaction (15.7, 16.0, and 16.9 MeV).

The measured ^{230}Th$(p, 2n)$ cross sections are lower than the cross sections calculated by TENDL 2019, although the

TABLE I. Experimentally measured cross sections for the ^{230}Th$(p, 2n)$, ^{230}Th$(p, 3n)$, and ^{232}Th(p, n) reactions.

Energy (MeV)	^{230}Th$(p, 2n)$ ^{229}Pa (σ, mb)	^{230}Th$(p, 3n)$ ^{228}Pa (σ, mb)	^{232}Th(p, n) ^{232}Pa (σ, mb)
16.9 ± 0.1	107 ± 15	23 ± 1.3	17.3 ± 1.0
16.0 ± 0.1	148 ± 9	1.6 ± 0.15	14.7 ± 0.8
15.7 ± 0.14	156 ± 16	2.7 ± 1.6	15.2 ± 0.7
14.9 ± 0.1	163 ± 32		12.0 ± 0.7
14.4 ± 0.1	182 ± 12		12.1 ± 0.7
14.1 ± 0.1	166 ± 32		11.7 ± 0.7

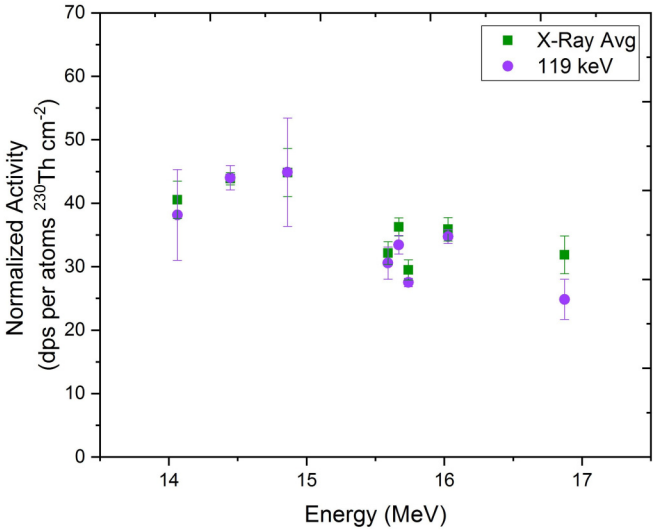

FIG. 4. Comparison of ^{229}Pa activity calculated via direct measurement of 119 keV line and x-ray analysis. The activities were normalized by the ^{230}Th atomic areal density of the original target.

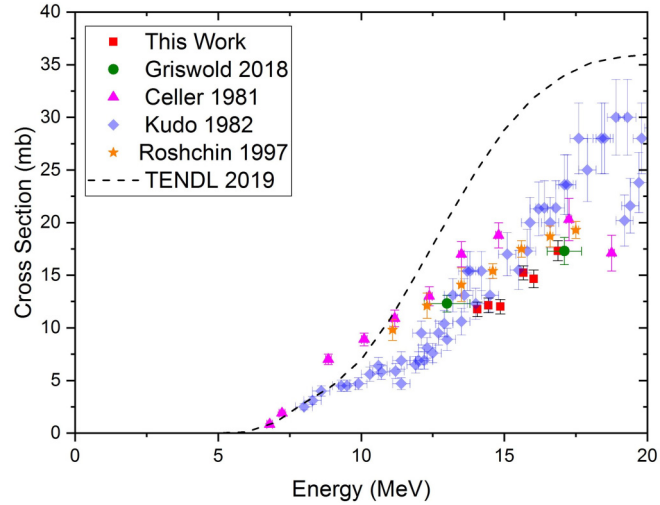

FIG. 5. Measured excitation function of the ^{232}Th(p, n) ^{232}Pa reaction from 16.8 to 14.1 MeV compared with the TENDL 2019 calculation and literature data. Cross-section error propagated from the standard deviation of several activity measurements. The point at 15.66 ± 0.15 MeV is an average over three measurements; the error on the cross section and the energy is given by the standard deviation.

measured peak appears to align well with the calculation, which puts it at 14 MeV [19]. The limited measurements of the ^{230}Th(p, 3n) reaction appear to be in good agreement with the TENDL calculation.

Based on the cross section shown in Fig. 3, the ^{230}Th(p, 2n) reaction is a reasonable method for ^{225}Ac production only if relatively large amounts of isotopically pure ^{230}Th were available, which could be obtained from the decay of ^{234}U or produced with isotope separation. As the activities required for TAT are in the range of 0.1 to 1.4 mCi per patient per dose [5], current methods of ^{225}Ac production are focused on the production of around ≈10 mCi ^{225}Ac/month [11]. With a target of 2 mg/cm^2 ^{230}Th (either mixed with ^{232}Th or isotopically pure), a 36 hour irradiation with a beam current of 1 μA would produce 80 μCi of ^{229}Pa but only 0.34 μCi of ^{225}Ac at its maximum activity (see Fig. S2 in the Supplemental Material [30]) due to the low alpha decay branching ratio (0.48%) [22]. The production of ^{229}Th via the decay of ^{229}Pa is insignificant (<0.1 nCi) due to the long ^{229}Th half-life ($t_{1/2}$ = 7340 years) (see Fig. S3 in the Supplemental Material [30]) [22]. Because the production of ^{229}Pa saturates around 36 hours, increasing the irradiation time does not significantly impact production. Increasing the beam current to 200 μA (reasonable for isotope production facilities [5,11]), increases the production to 16 040 μCi of ^{229}Pa but still only 9 nCi of ^{229}Th and a maximum of 68 μCi of ^{225}Ac. Increasing production by increasing the target thickness would require a significant supply of isotopically pure ^{230}Th because the size of a mixed ^{230}Th / ^{232}Th target obtained from natural sources, such as that used in this work, containing sufficient ^{230}Th would be impossibly large (>10 g/cm^2).

An advantage of production with the ^{230}Th(p, 2n) reaction, if it were feasible to scale up, would be high isotopic purity of the resultant ^{225}Ac. There are limited routes to other actinium isotopes even with mixed ^{230}Th / ^{232}Th targets. The in-growth of ^{226}Ac via ^{230}Pa alpha decay (0.0032%) [22] is minor and has been neglected in past studies [5]. At low proton energies, there would be no production of ^{224}Ac (via the decay of ^{228}Pa) and ^{227}Ac would mainly arise from the decay of ^{231}Pa from the ^{232}Th(p, 2n) reaction because the (p, γ) and (p, α) reactions on ^{230}Th are predicted to be negligible [19]. Due to the long half-life of ^{231}Pa, the production of ^{227}Ac is low even with a considerable quantity of ^{232}Th. The irradiation of 24 mg/cm^2 mixed ^{230}Th / ^{232}Th (with an isotope ratio similar to that of the thorium material used in this work) for 36 hours at 200 μA would result in the production of 16 040 μCi of ^{229}Pa, which decays to 68 μCi of ^{225}Ac in ≈40 days, but only 63 nCi ^{231}Pa, which decays to 0.2 nCi ^{227}Ac in the same time. This gives a ^{227}Ac / ^{225}Ac ratio of 3.25 × 10^{-6}, which is significantly better than current ^{227}Ac / ^{225}Ac ratios from production at the Isotope Production Facility (IPF) and Brookhaven Linac Isotope Producer (BLIP), 1.8 × 10^{-3} and 2.07 × 10^{-3}, respectively [9].

The results for the measurement of the ^{232}Th(p, n) excitation function, which was used to validate the experimental conditions, are shown in Fig. 5. The ^{232}Pa activity was determined from its 150, 388, 581, 819, and 867 keV lines as well as the 969.32 keV line for measurements below 15 MeV where there was no production of ^{228}Pa, which has a γ-ray line with a similar energy at 968.97 keV. The activity was determined from the average activity of these five (or six) lines in three spectra taken within the first 24 hours post-irradiation; error is from the standard deviation. The measurement agrees well with the literature data for this cross section in the relevant energy range.

B. Half-life measurements

For each protactinium sample, the 119 keV γ-ray line from ^{229}Pa was followed over several half-lives to ensure it was

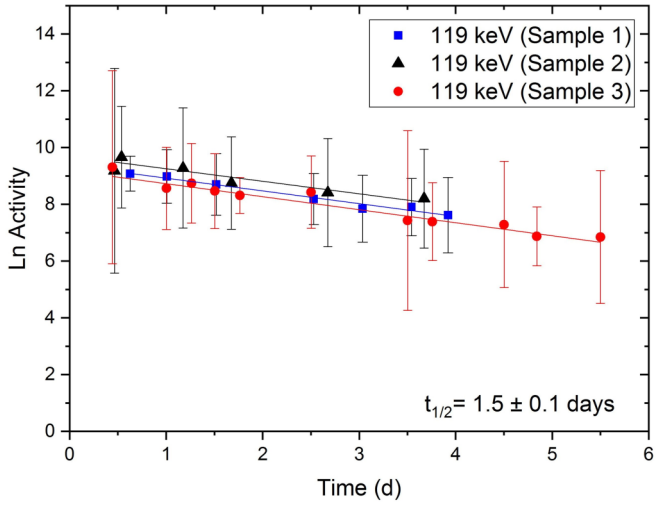

FIG. 6. Measurement of the ^{229}Pa half-life from the 119 keV γ-ray line for three protactinium samples. Error is statistical counting error. Least squares fit done with the program ORIGIN 2018 (OriginLab).

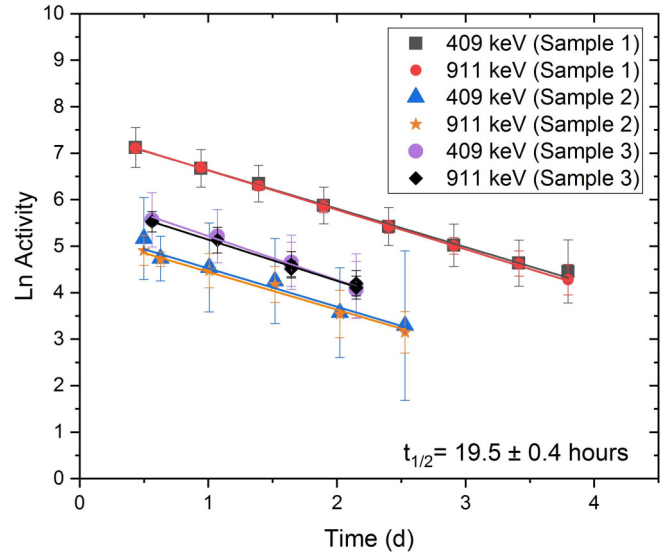

FIG. 7. Measurement of the ^{228}Pa half-life from the 409 and 911 keV γ-ray lines for three protactinium samples. Error is statistical counting error. Least squares fit done with the program ORIGIN 2018 (OriginLab).

decaying with the appropriate half-life. For the three samples with the highest ^{229}Pa activity, the half-life was measured based on this γ-ray line (see Fig. 6). The average measured half-life was 1.5 ± 0.1 days with error propagated from the statistical counting error. This agrees well with the half-life from the evaluated nuclear (1.50 ± 0.05 days [22]) as well as the recent measurement by Griswold *et al.*, of 1.55 ± 0.01 days [11].

The half-life of ^{228}Pa was also measured from three samples using two γ-ray lines: 409 and 911 keV. While ^{228}Pa also has a 463.00 keV line with a high intensity, this line was not used because there is an interference from ^{230}Pa, which has a 463.59 keV γ-ray line. The average measured half-life was 19.5 ± 0.4 hours (Fig. 7), which is smaller than the half-life given in the evaluated nuclear data (22 ± 1 hours) [34,35].

The nuclear data for the half-life of ^{228}Pa were last evaluated in December 2012 by the International Network of Nuclear Structure and Decay Data Evaluators [34]. The half-life in the Evaluated Nuclear Structure Data File (ENSDF) is 22 ± 1 hours [34], which is based on the measurement in Ref. [36]. Another measurement of 29 ± 1 hours from Ref. [37] is noted in ENSDF, but was not included in the final half-life assessment. The measurement from Ref. [36] was made in 1951 based on alpha pulse analysis with an argon ionization chamber using a ^{228}Pa sample known to be contaminated with the slightly longer lived ^{229}Pa. Furthermore, Ref. [36] notes that the two isotopes cannot be easily differentiated with alpha pulse analysis as their alpha emission energies are similar. Therefore, the decrease in the measured half-life is likely explained by the use of γ-ray rather than alpha spectrometry as the value from Ref. [36] may be an overestimate due to the presence of ^{229}Pa in the sample and the difficulties in resolving the alpha emission peaks of ^{228}Pa and ^{229}Pa.

IV. CONCLUSION

Excitation functions are reported for the first time in the literature for the ^{230}Th$(p, 2n)$ and ^{230}Th$(p, 3n)$ reactions from 14.1 to 16.9 MeV. The ^{232}Th(p, n) reaction was measured as well to verify the experimental conditions. The measured excitation functions were compared with the calculations from TENDL 2019 and there is reasonably good agreement, although the measured ^{230}Th$(p, 2n)$ cross sections are lower than the calculation. This was expected because TENDL calculations for ^{232}Th(p, xn) reactions also tend to be slightly higher (Fig. 5) than the measured data. The peak measured cross section for the ^{230}Th$(p, 2n)^{229}$Pa reaction was 182 ± 12 mb at 14.4 ± 0.1 MeV, although the measurements from 14.1 to 14.9 MeV were all within error, so the peak cannot be determined conclusively. This aligns well with the peak calculated by TENDL 2019 of 14 MeV [19]. Based on this cross section, production of ^{225}Ac via the ^{230}Th$(p, 2n)$ reaction is only feasible with a significant amount of isotopically pure ^{230}Th as mixed ^{230}Th / ^{232}Th targets from natural sources with sufficient levels of ^{230}Th would be impractically large.

Half-life measurements for ^{229}Pa and ^{228}Pa are presented, the measured half-lives are 1.5 ± 0.1 days and 19.5 ± 0.4 hours, respectively. The measured half-life for ^{229}Pa agrees well with the literature values. The measured half-life for ^{228}Pa is slightly smaller than the half-life given in ENSDF, likely due to how the half-life of ^{228}Pa was historically measured.

ACKNOWLEDGMENTS

This study was performed under the auspices of the U.S. Department of Energy by Lawrence Livermore National Laboratory under Contract DE-AC52-07NA27344. This work was funded by the LLNL Livermore Graduate

Research Scholar Program. This material is based upon work supported by the Department of Energy National Nuclear Security Administration through the Nuclear Science and Security Consortium under Award No. DE-NA0003180. The authors would like to thank the CAMS facility staff at LLNL, particularly Scott Tumey, for providing beam time as well as Keenan Thomas and Todd Wooddy for assisting with γ-ray spectrometry.

[1] J. Elgqvist, S. Frost, J. Pouget, and P. Albertsson, The potential and hurdles of targeted alpha therapy-clinical trials and beyond, Front. Oncol. **3**, 324 (2013).

[2] A. Morgenstern, F. Bruchertseifer, and C. Apostolidis, Bismuth-213 and Actinium-225-generator performance and evolving therapeutic applications of two generator-derived alpha-emitting radioisotopes, Curr. Radiopharm. **5**, 221 (2012).

[3] C. Kratochwil, F. Bruchertseifer, H. Rathke, M. Hohenfellner, F. Giesel, U. Haberkorn, and A. Morgenstren, Targeted alpha therapy of metastatic castration-resistant prostate cancer with ^{225}Ac-PSMA-617: Swimmer-plot analysis suggests efficacy regarding duration of tumor control, J. Nucl. Med. **59**, 795 (2018).

[4] P. Borchardt, R. Yuan, M. Miederer, M. McDevitt, and D. Scheinberg, Targeted Actinium-225 *in vivo* generators for therapy of ovarian cancer, Cancer Res. **63**, 5084 (2003).

[5] A. Morgenstern, C. Apostolidis, C. Kratochwil, M. Sathekge, L. Krolicki, and F. Bruchertseifer, An overview of targeted alpha therapy with ^{225}Actinium and ^{213}Bismuth, Curr. Radiopharm. **11**, 200 (2018).

[6] A. Robertson, C. F. Ramogida, P. Schaffer, and V. Radchenko, Development of ^{225}Ac radiopharmaceuticals: TRIUMF perspectives and experiences, Curr. Radiopharm. **11**, 156 (2018).

[7] R. A. Aliev, S. V. Ermolaev, A. N. Vasiliev, V. S. Ostapenko, E. V. Lapshina, B. L. Zhuikov, N. V. Zakharov, V. V. Pozdeev, V. M. Kokhanyuk, B. F. Myasoedov, and S. N. Kalmykov, Isolation of medicine-applicable Actinium-225 from thorium targets irradiated by medium-energy protons, Solvent Extr. Ion Exch. **32**, 468 (2014).

[8] C. Kratochwil, F. L. Giesel, F. Bruchertseifer, W. Mier, C. Apostolidis, R. Boll, K. Murphy, U. Haberkorn, and A. Morgenstern, ^{213}Bi-DOTATOC receptor-targeted alpha-radionuclide therapy induces remission in neuroendocrine tumours refractory to beta radiation: A first-in-human experience, Eur. J. Nucl. Med. Mol. Imaging **41**, 2106 (2014).

[9] J. Griswold, D. Medvedev, J. Engle, R. Copping, J. Fitzsimmons, V. Radchenko, J. Cooley, M. Fassbender, D. D. L. Denton, K. Murphy, A. Owens, E. E. R. Birnbaum, K. John, F. Nortier, D. Stracener, L. Heilbronn, F. Mausner, and S. Mirzadeh, Large scale accelerator production of ^{225}Ac: Effective cross sections for 78–192 MeV protons incident on ^{232}Th targets, Appl. Radiat. Isot. **118**, 366 (2016).

[10] J. Engle, J. Weider, B. Ballard, M. Fassbender, L. Hudston, K. Jackman, D. Dry, L. Wolfsburg, L. Bitteker, J. Ullman, M. Gulley, C. Pillai, G. Goff, E. Birnbaum, K. John, S. Mashnik, and F. Nortier, Ac, La, and Ce radioimpurities in ^{225}Ac produced in 40–200 MeV proton irradiations of thorium, Radiochim. Acta **102**, 569 (2014).

[11] J. R. Griswold, C. U. Jost, D. W. Stracener, S. H. Bruffey, D. Denton, M. Garland, L. Heilbronn, and S. Mirzadeh, Production of ^{229}Th for medical applications: Excitation functions of low-energy protons on ^{232}Th targets, Phys. Rev. C **98**, 044607 (2018).

[12] B. Zhuikov, S. Kalmykov, S. Ermolaev, R. Aliev, V. Kokhanyuk, V. Matushko, G. Tananaev, and B. Myasoedov, Production of ^{225}Ac and ^{223}Ra by irradiation of Th with accelerated protons, Radiochemistry (Moscow, Russ. Fed.) **53**, 73 (2011).

[13] J. Boldeman and R. Walsh, $\bar{\nu}_p$ for sub-barrier fission in ^{230}Th, Phys. Lett. B **62**, 149 (1976).

[14] G. Yuen, G. Rizzo, A. Behkami, and J. Huizenga, Fragment angular distributions of the neutron-induced fission of ^{230}Th, Nucl. Phys. A **171**, 614 (1971).

[15] A. Sicre, T. Benfoughal, B. Bruneau, M. Asghar, G. Barreau, F. Caitucoli, T. Doan, G. James, and B. Leroux, Fission-fragment angular distributions for ^{230}Th(n, f) in the vicinity of the 715 keV resonance, Nucl. Phys. A **445**, 37 (1985).

[16] A. Levona, J. de Boera, G. Grawa, R. Hertenberger, D. Hofer, J. Kvasil, A. Losch, E. Muller-Zanotti, M. Wurkner, H. Baltzer, V. Grafen, and C. Gunther, The nuclear structure of ^{229}Pa from the ^{231}Pa(p,t)^{229}Pa and ^{230}Th(p,2nγ)^{229}Pa reactions, Nucl. Phys. A **576**, 267 (1994).

[17] V. Grafen, B. Ackermann, H. Baltzer, T. Bihn, C. Günther, J. de Boer, N. Gollwitzer, G. Graw, R. Hertenberger, H. Kader, A. Levon, and A. Lösch, Does a $5/2^+$-$5/2^+$ ground-state parity doublet exist in ^{229}Pa? Phys. Rev. C **44**, R1728(R) (1991).

[18] D. Burke, P. Garrett, and T. Qu, Levels in ^{227}Ac populated in the ^{230}Th(p, α) reaction, Nucl. Phys. A **724**, 274 (2003).

[19] A. Koning, D. Rochman, J. Sublet, N. Dzysiuk, M. Fleming, and S. van der Marck, Tendl: Complete nuclear data library for innovative nuclear science and technology, Nucl. Data Sheets **155**, 1 (2019).

[20] Q-value calculator, National Nuclear Data Center (NNDC) Brookhaven National Laboratory (2019), accessed: 2020-11-16.

[21] M. Wang, G. Audi, F. Kondev, W. Huang, S. Naimi, and X. Xu, The AME2016 atomic mass evaluation (II). Tables, graphs and references, Chin. Phys. C **41**, 030003 (2017).

[22] National Nuclear Data Center (NNDC) Brookhaven National Laboratory (2019), accessed: 2020-11-16.

[23] N. Nerozin, S. Khamianov, V. Shapovalov, and S. Tkachev, Current status and perspective of Actinium-225 production at JSC SSC RF-IPPE, in *Report on Joint IAEA-JRC Workshop: Supply of Actinium-225* (International Atomic Energy Agency (IAEA) and the Joint Research Centre (JRC) of the European Commission, Vienna, Austria, 2018).

[24] K. Kmak, D. Shaughnessy, and J. Vujic, Separation of thorium from uranium ore, J. Radioanal. Nucl. Chem. **323**, 931 (2020).

[25] J. Meija, T. Coplen, M. Berglund, W. Brand, P. D. Bievre, M. Groning, N. Holden, J. Irrgeher, R. Loss, T. Walczyk, and T. Prohaska, Atomic weights of the elements 2013 (IUPAC Technical Report), Pure Appl. Chem. **88**, 265 (2016).

[26] S. Turner, P. van Calsteren, N. Vigier, and L. Thomas, Determination of thorium and uranium isotope ratios in low concentration geological materials using a fixed multi-collector-icpms, J. Anal. At. Spectrom. **16**, 612 (2001).

[27] J. Ziegler, J. Biersack, and U. Littmark, *The Stopping and Range of Ions in Matter* (Pergamon Press, New York, 1985).

[28] A. Roshchin, S. Yavshits, V. Jakovlev, E. Karttunen, J. Aaltonen, and S. Heselius, Cross sections of nonfission

reactions induced in Th-232 by low-energy proton, Phys. At. Nucl. **60**, 1941 (1997).

[29] J. Szerypo, B. Szweryn, P. Hornshoj, H. L. Nielsen, and M. Luontama, Radiative capture of protons by the deformed nuclide Th-232, Z. Phys. A **324**, 439 (1986).

[30] See Supplemental Material at http://link.aps.org/supplemental/10.1103/PhysRevC.103.034610 for table of relevant gamma-ray lines, simplified decay scheme of ^{229}Pa electron capture decay and Bateman plots for the in-growth of ^{229}Th, ^{225}Ra, and ^{225}Ac into ^{229}Pa.

[31] R. Gunnink and J. Niday, Computerized quantitative analysis of gamma-ray spectrometry, UCRL-51061, Livermore National Laboratory, Livermore.

[32] N. Soppera, E. Dupont, and M. Fleming, Janis books (OECD NEA Data Bank, 2020).

[33] ENSDF nuclear data sheets: ^{229}Pa ϵ decay, Nucl. Data Sheets **109**, 2657 (2008).

[34] ENSDF nuclear data sheets: ^{228}Pa, Nucl. Data Sheets **116**, 163 (2014).

[35] S. Chu, L. Ekstrom, and R. Firestone, The Lund/LBNL nuclear data search, Lawrence Berkeley National Laboratory (1999), accessed: 2020-11-16.

[36] W. Meinke, A. Ghiorso, and G. Seaborg, Artificial chains collateral to the heavy radioactive families, Phys. Rev. **81**, 782 (1951).

[37] C. Gerschel, M. Pautrat, R. Ricci, J. Vanhorenbeeck, and J. Teillac, Etude des Series α de Protactinium 227, 228, 229 et 230, *Phys. Nucl. Annuaire 1962-63* (Faculte Sci. L'Univ. Paris Inst. Rad., 1964), p. 47.